Output Voltage Regulation of IPOS Modular Dual Active Bridge DC/DC Converters using Sliding Mode Control

Sangmin Lee, Yoon-Cheul Jeung and Dong-Choon Lee
Department of Electrical Engineering, Yeungnam University
280 Daehak-Ro, Gyeongsan, Gyeongbuk, 38541 Korea
eternalpogo@naver.com, jyclb@ynu.ac.kr, dclee@yu.ac.kr

***Abstract*— In this paper, a novel output voltage control scheme for the input-parallel output-series (IPOS) modular dual active bridge (DAB) DC/DC converter is proposed, based on the hierarchical sliding mode control (HSMC). The proposed controller provides a balancing control of output voltages of individual modules as well as the overall DC bus voltage regulation even if there is a parameter mismatch. Also, the control performance is less sensitive to parameter perturbation by applying the sliding mode control theory. The validity of the proposed control method is verified by experimental results.**

Keywords— dual active bridge, DC/DC converter, sliding mode control

I. INTRODUCTION

Recently, the modular DC/DC converters have attracted great attention for industrial applications such as DC transmission and distribution systems, solid state transformers, and energy storage systems (ESS) [1]-[3]. In the modular structure, the entire DC/DC converter can be controlled through the control of individual modules. In addition, it is possible to configure the four types by series and parallel connections of the input and output, respectively. According to the requirements of the system, the converter can be easily expanded . Also, the reliability of the system can be improved.

The dual active bridge (DAB) DC/DC converter is one of isolated DC/DC converters, which has the advantages of high efficiency through soft switching and bidirectional power flow [4],[5]. Therefore, it can be employed as a module for high power modular DC/DC converters.

This paper focuses on the input-parallel output-series (IPOS) modular DAB converter which can be used for the two-stage DC/DC conversion systems [6],[7]. The modular-type DAB converter is shown in Fig. 1, where the number of module is two. It is noted that the modular converter system can be expanded by adding more modules. The role of the modular DAB converter is to control the power between the low-voltage DC (LVDC) bus and medium-voltage DC (MVDC) bus for two-stage DC/DC conversion systems. In this case, the LV and MV sides of the DAB converter modules are connected in parallel and series, respectively.

In the case of the output-series connection, the output voltages of each module are often unbalanced due to the parameter mismatch in internal resistance, transformer turn ratio and leakage inductance even if the overall DC bus output voltage is well controlled. Therefore, it is necessary to control the output voltages of individual modules to be balanced.

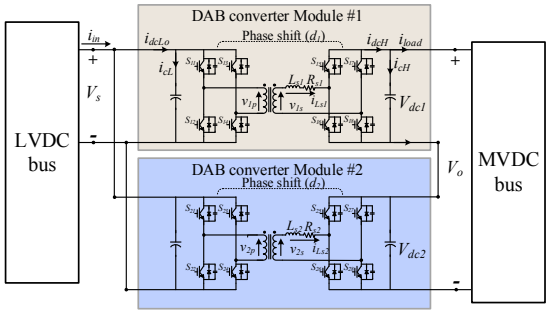

Fig. 1. IPOS modular DAB converter.

To balance the voltages of individual modules, the droop control-based output voltage control was proposed [8],[9]. Basically, the DC bus voltage controller is applied to maintain the MVDC voltage. In addition, the voltage references of the individual modules are adjusted by the droop gain with output current feedback. Although this method is simple to implement and control, an additional current sensor is required for each DAB converter module. In [10]-[12], the voltages of the individual modules are controlled based on the master-slave control structure. In this method, the references of the output voltages of the slave modules are generated by the controller of the master module. At the same time, the slave controller is used for each slave module, which controls its output voltage to be equal to that of the master module. Then, the output voltages of individual modules are balanced well. However, the drawback of this method is low reliability and complexity. On the other hand, the model predictive control (MPC) [13] was suggested for the voltage balancing of individual modules with linear output voltage controller. In this method, the control performance of the DAB converter is affected by the inaccurate parameter.

In this paper, a novel output voltage controller for the modular DAB DC-DC converters is proposed, based on sliding mode control theory. First, the nonlinear model of the converter is derived, where the single phase-shift modulation (SPSM) is applied. Next, a voltage controller is designed based on the hierarchical sliding mode control (HSMC) theory. Then, the effect of parameter mismatch on the control performance is investigated. The validity of the proposed control scheme is verified by experimental results.

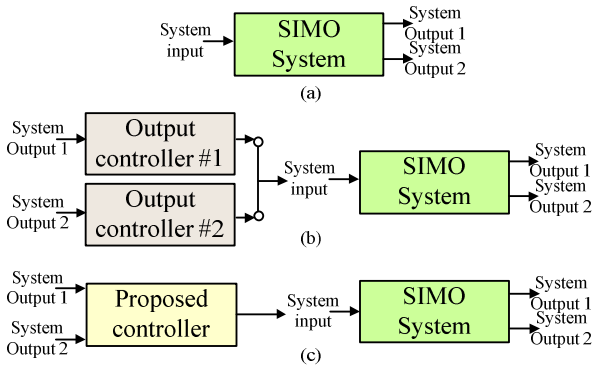

Fig. 2. Configuration of SIMO systems and controller. (a) SIMO system. (b) General controller of SIMO system. (c) Proposed controller of SIMO system.

II. Configuration and Modeling of IPOS Modular DAB Converters

The model of the DAB converter is required to design the nonlinear controller. To derive a model of the IPOS modular DAB converter, the model of the single DAB converter module is needed.

A. Configuration of modular DAB converters

Fig. 1 shows the two DAB modules, where the input terminals of the DAB modules are connected in parallel to the LVDC bus and the output terminals of the DAB modules are connected in series, which are connected to the MVDC bus. The DAB converter module consists of one high-frequency transformer, four IGBT legs, where V_s is the input voltage, V_o is the output voltage, and V_{dc1} and V_{dc2} are the output voltages of each module. The d_1 and d_2 are the phase shift ratios of the primary and secondary voltages of the transformer for each module.

The input-parallel output-series (IPOS) modular converter is a single-input multi-output (SIMO) system. The SIMO system is shown in Fig. 2(a). The single input is related to the phase shift ratio which is applied to each module. The multi-output constitutes the total voltage (MCDC bus voltage) and output voltages of each module. Also, a single DAB module is an SIMO system since the output of the single DAB module affects its output voltage and the (DC bus voltage. In general, to control the SIMO system, the all outputs are required in the output controllers as shown in Fig. 2(b). The existing methods follow this approach, which increase the complexity when multiple DAB modules are employed. However, the proposed controller has a single control input for multiple outputs of system using only one controller as shown in Fig. 2(c). Then. the DC bus voltage and output voltages of modules can be controlled by the individual module controllers.

B. Single phase shift modulation of IPOS DAB converters

In this work, the single phase shift modulation (SPSM) is applied to control the IPOS DAB converter. Fig. 3 shows the waveforms of the SPSM in the ideal condition where the carrier waveforms of the DAB modules are identical and the transformer turn ratio is one to one. The output power is

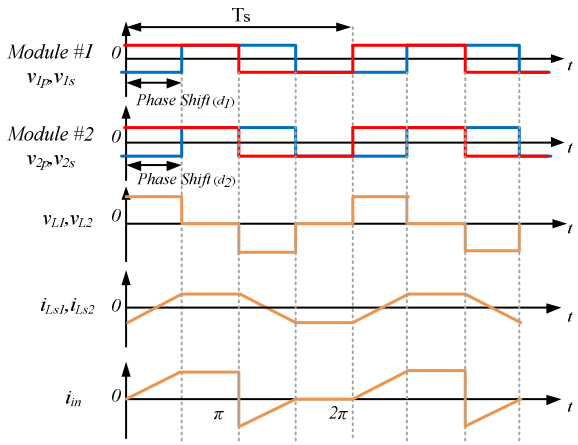

Fig. 3. Operating waveform of IPOS modular DAB converter for SPSM.

controlled by the phase shift ratio between v_{1p} and v_{1s}, which are the primary and secondary voltages of the transformer, respectively. In the operation of the SPSM, all switches of the DAB converter are operated at a fixed duty ratio of 0.5, and the upper and lower switches in one leg are operated complementarily. The average output power of the single DAB module #1 is given by [14],[15]

$$P_o = N\frac{v_{1p}v_{1s}}{2f_sL_{s1}}d_1(1-d_1) \tag{1}$$

where, N is the transformer turn ratio (v_{1s}/v_{1p}), f_s is the switching frequency, and d_1 is the phase-shift ratio of module #1. The total output power of the IPOS modular DAB converter is N_m times that of the individual modules. where N_m is the number of modules.

C. Modeling of DAB converter modules

The normalized state-space model of the output voltage for the DAB converter based on the SPSM has been derived in Ref. [16]. In this work, only the fundamental component ($k=0$) is considered for simplicity since the sliding mode control is robust to the model uncertainty of the system [17],[18]. Then,

$$\begin{aligned}\frac{d}{dt}V_{dc}(t) &= -\frac{8}{C_{out}\pi^2}\frac{\cos\{\varphi_z(0)\}}{|z(0)|}V_{dc}(t)\\ &+\frac{8}{C_{out}\pi^2}\frac{Nv_p(t)}{|z(0)|}\cos\{\delta-\varphi_z(0)\}\\ &-\frac{i_{Load}(t)}{C_{out}}\end{aligned} \tag{2}$$

where V_{dc} is the output voltage, C_{out} is the output capacitance, v_p is the primary voltage of transformer, i_{Load} is the load current, R_s is the internal resistance of transformer and inductor, L_s is the leakage inductance, δ is the phase shift angle. The impedance, $|z(0)|$, and the impedance angle, $\varphi_z(0)$, of transformer are expressed as, respectively

$$|z(0)| = \sqrt{R_s^2+(\omega_sL_s)^2} \tag{3}$$

$$\varphi_z(0) = \tan^{-1}\left(\frac{\omega_s L_s}{R_s}\right) \tag{4}$$

The input variable of the system can be selected as

$$u = \cos\{\delta - \varphi_z(0) + \delta_0\} \tag{5}$$

Also, the initial value of the phase shift angle can be selected as

$$\delta_0 = -\pi/2 + \varphi_z(0) \tag{6}$$

Then, the input u is obtained as

$$u = \sin\{\delta\} \tag{7}$$

D. Modeling of IPOS modular DAB converters

In this section, the mathematical model of the IPOS modular DAB converter is derived. From (2), the overall DC output voltages of the IPOS modular DAB converter and the individual module #1 can be expressed in a state-space form in (8) and (9), respectively, if there is no parameter mismatch between the two modules,

$$\dot{x}_1 = f_1(x_1) + g_1(x_1)u_1 + E_1 \tag{8}$$

$$\dot{x}_2 = f_2(x_2) + g_2(x_2)u_2 + E_2 \tag{9}$$

where x_1 is the overall output voltage of the IPOS modular DAB converter, x_2 is the output voltage of the individual module #1, and

$$f_1(x_1) = -\frac{8}{C_{out}\pi^2}\frac{\cos\{\varphi_z(0)\}}{|z(0)|}V_o$$

$$g_1(x_1) = \frac{8}{C_{out}\pi^2}\frac{N}{|z(0)|}V_o$$

$$E_1 = 2\{-\frac{i_{Load}(t)}{C_{out}}\}$$

$$u_1 = \sin\{\delta_1\}$$

$$f_2(x_2) = \{-\frac{8}{C_{out}\pi^2}\frac{\cos\{\varphi_z(0)\}}{|z(0)|}\}V_{dc1}$$

$$g_2(x_2) = \{\frac{8}{C_{out}\pi^2}\frac{N}{|z(0)|}\}V_{dc1}$$

$$g_2(x_2) = \{\frac{8}{C_{out}\pi^2}\frac{N}{|z(0)|}\}V_{dc1}$$

$$u_2 = \sin\{\delta_2\}$$

The mathematical model of module #2 can be obtained with the same technique as above.

III. Design of Hierarchical Sliding Mode Contorollers

A. Basic theory of sliding mode control

The sliding mode control is a control technique that allows the system to contact the predetermined sliding surface regardless of the initial conditions given in the system. The advantage of the SMC is that the system is less sensitive to system perturbations, external disturbances and parameter mismatches [19].

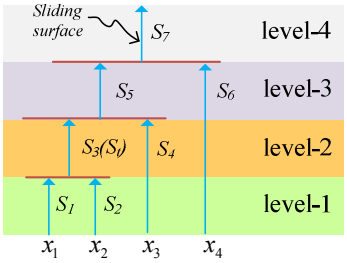

Fig. 4. Structure of hierarchical sliding surfaces.

The SMCs have three steps of control mechanisms. In the first step, the state variable is controlled to reach the selected surface regardless of its initial position. In the next step, the state variable is controlled to stay on the sliding surface. The last step is to control the state variables to converge to the equilibrium point along the sliding surface.

The basic design procedure of sliding mode control is as followings. Consider the nonlinear state-space equation as

$$x' = f(x) + g(x)u + E \tag{10}$$

where $f(x)$ and $g(x)$ are the nonlinear functions, x is a state, x' represents the derivative of the state, u is the control input, E is the disturbance. The sliding surface can be selected as

$$s = e - \int e \tag{11}$$

where e is the regulation error. The function of $sgn(s)$ is applied to the derivative term of (11). The state vector approaches to the sliding surface by using the "*sgn*" function.

$$s' = f(x) + g(x)u + E + e = \mathrm{sgn}(s) \tag{12}$$

The output of *sgn* function is defined by sliding surface as

$$\mathrm{sgn}(s) = \begin{cases} 1 & if \quad s > 0 \\ 0 & if \quad s = 0 \\ -1 & if \quad s < 0 \end{cases} \tag{13}$$

The final control input of basic SMC can be expressed as

$$u = \frac{-(f(x) + E + e) + \mathrm{sgn}(s)}{g(x)} \tag{14}$$

The existence condition of the control system is guaranteed by utilizing the Lyapunov function which is defined as

$$V = \frac{1}{2}S^2 \tag{15}$$

If the derivative of Lyapunov function is negative definite, that is

$$V' = SS' < 0 \tag{16}$$

then, the existence condition of the sliding mode is satisfied.

B. Design of hierarchical sliding mode controller

In this section, the hierarchical sliding mode controller is designed for regulating the output voltage of the ISOP converter as well as balancing the voltages of the DAB converter modules.

The HSMC is an SMC techniques for SIMO systems [20],[21]. Fig. 4 shows the structure of the hierarchical sliding surfaces, where the higher-level surface contains the lower-level surfaces. Then, the single input can control the multiple output variables.

First, the equivalent control inputs of the level-1 are derived as follows. The sliding surfaces of level-1 for module #1 are selected as

$$s_1 = c_1 e_1 + c_2 \int e_1 \tag{17}$$

$$s_2 = c_3 e_2 + c_4 \int e_2 \tag{18}$$

where e_1 is the regulation error of overall output voltage, e_2 is that of the single module and c_1, c_2, c_3, c_4 are the gains of the HSMC. Taking a derivative of (17),

$$s_1^{'} = c_1 e_1^{'} + c_2 e_1 \tag{19}$$

where $s_1^{'}$ and $e_1^{'}$ represent the derivative of the sliding surface and regulation error, respectively. From (5), the derivative of the regulation error can be expressed as

$$e_1^{'} = x_1^{'} - x_{1d}^{'} = f_1(x_1) + g_1(x_1)u_1 + E_1 \tag{20}$$

Substituting (20) into (19),

$$s_1^{'} = c_1(f_1(x_1) + g_1(x_1)u_1 + E_1) + c_2 e_1 \tag{21}$$

The u_1 can be obtained by setting the derivative of the sliding surfaces s_1 as zero. Then, the control input (u_1) of the sliding surface of level-1(s_1) is obtained as

$$u_1 = \frac{-c_1 f_1(x_1) - c_1 E_1 - c_2 e_1}{c_1 g_1(x_1)} \tag{22}$$

In the same way, the control input(u_2) to the s_2 sliding surface of level-1 is obtained as

$$u_2 = \frac{-c_3 f_2(x_2) - c_3 E_2 - c_4 e_2}{c_3 g_2(x_2)} \tag{23}$$

Second, the equivalent control inputs of the level-2 are derived as follows. The sliding surface of level-2(S_t) can be selected as

$$S_t = s_1 + \alpha s_2 \tag{24}$$

where α is the control gain. The equivalent control input (u_{eq}^*) in (24) can be selected as [20]

$$\begin{aligned} u_{eq}^* &= u_1 + u_2 + u_{sw} \\ &= \frac{-c_1 f_1(x_1) - c_1 E_1 - c_2 e_1}{c_1 g_1(x_1)} + \frac{-c_3 f_2(x_2) - c_3 E_2 - c_4 e_2}{c_3 g_2(x_2)} + u_{sw} \end{aligned} \tag{25}$$

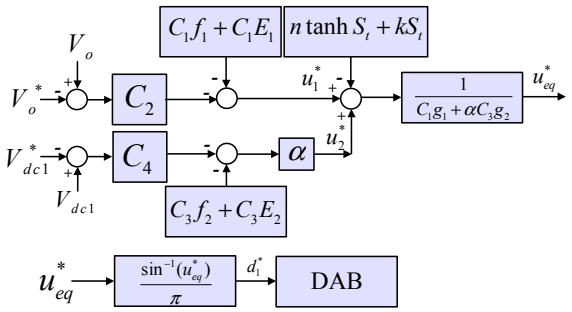

Fig. 5. Block diagram of HSMC for single DAB converter module.

The condition for the state variable to reach the sliding surface of level-2 can be selected as

$$S_t^{'} = -n\,\mathrm{sgn}(S_t) - mS_t \tag{26}$$

where n and m are the HSMC gains. To reduce the chattering effect, the "*sgn*" function can be replaced by *tanh* [7].

$$\mathrm{sgn}(S_t) = \tanh(S_t) \tag{27}$$

Then, the function for reaching the selected sliding surface of level-2 (u_{sw}) is obtained as

$$u_{sw} = \frac{-c_1 g_1(x_1) u_2 - \alpha c_3 g_2(x_2) u_1 - n \tanh(S_t) - mS_t}{c_1 g_1(x_1) + \alpha c_3 g_2(x_2)} \tag{28}$$

From (25) and (28), the equivalent control input for level-2 is derived as

$$\begin{aligned} u_{eq}^* = \frac{1}{c_1 g_1(x_1) + \alpha c_3 g_2(x_2)} [&-(c_1 f_1(x_1) + c_1 E_1 + c_2 e_1) \\ &- \alpha(c_3 f_2(x_2) + c_3 E_2 + c_4 e_2) - (n \tanh S_t + mS_t)] \end{aligned} \tag{29}$$

Finally, from (7) and (29), the phase shift ratio of the DAB converter is obtained as

$$d^* = \frac{\sin^{-1}(u_{eq}^*)}{\pi} \tag{30}$$

Fig. 5 shows the control block diagram of the single DAB converter module.

C. Existence condition of HSM

The existence condition of the HSM can be verified by substituting (24) and (26) into (16) as

$$V^{'} = S_t S_t^{'} = (s_1 + \alpha s_2)(-n\,\mathrm{sgn}(S_t) - mS_t) \tag{31}$$

If the gains n, m and α are the positive constant, then Lyapunov function is always negative. It means that the existence condition of the HSMC is satisfied.

IV. Experimental Results

The system parameters for hardware experiments are listed in the Table 1 and 2. The experimental setup of modular DAB converter is shown in Fig. 6. The input and output voltages of the modular DAB converter are 75 V and 150 V, respectively.

TABLE I. PARAMETERS OF MODULAR DAB CONVERTER

Parameters	Value
LVDC bus voltage (Input Voltage of IPOS converter)	75 V
MVDC bus voltage (Output Voltage of IPOS converter)	150 V
Number of modules	2

TABLE II. PARAMETERS OF TWO DAB MODULES

Parameters	Value
Input DC voltage(V_s)	75 V
Output DC voltage ($V_{dc1,2}$)	75 V
Transformer turn ratio (Primary : Secondary)	1 : 1
Equivalent series inductances of transformer leakage and auxiliary (L_{s1}, L_{s2})	200uH,250uH
Output capacitance	200uF
Switching frequency	5 kHz

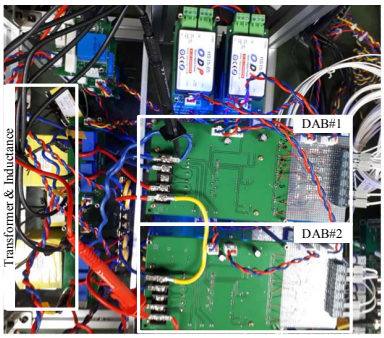

Fig. 6. Experimental setup (IPOS Modular DAB DC/DC converter).

To verify the robustness of the proposed method, the case of inductance mismatch between two DAB modules (L_{s1} = 200μH and L_{s2} = 250μH) is considered.

The HSM controller gains (c_1, c_3 = 1.02×10^{-5}, c_2, c_4 = 5.1×10^{-3}, n = 0.001, m = 108) have been determined by a trial and error, which satisfy the existence condition of sliding surfaces. For performance comparison, the PI controller is adopted, where the PI gains are determined based on small signal analysis [16], which are given by

PI-1 : k_p = 1.11×10^{-4}, k_i = 0.0697 (bandwidth : 38 rad/sec)

PI-2 : k_p= 3.33×10^{-4}, k_i = 0.2092 (bandwidth : 100 rad/sec)

PI-3 : k_p= 5.55×10^{-4}, k_i = 0.3486 (bandwidth : 150 rad/sec)

Fig. 7 shows the control performance of the HSMC for the different inductance case, where the load is changed from 380 W to 600 W and back to 380 W. The waveform of total DC output voltage is shown in Fig. 7(a). The DC output voltage follows its reference well. The overshoot and undershoot in the transient condition are less than 10%. Fig. 7(b) shows the output voltage of the two DAB modules, which are well controlled as 75 V. Fig. 7(c) shows the phase shift ratio of the

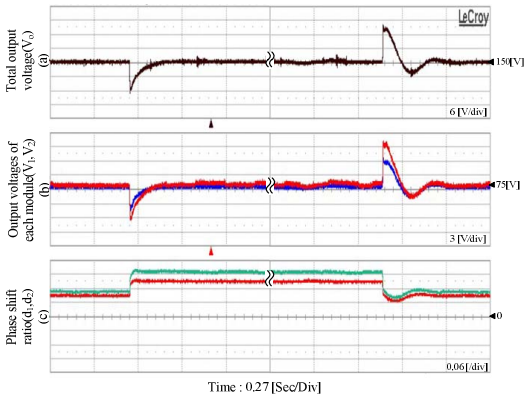

Fig. 7. HSM control performance under different inductance conditions, (a) Overall DC output voltage. (b) Output voltages of two modules. (c) Phase shift ratio.

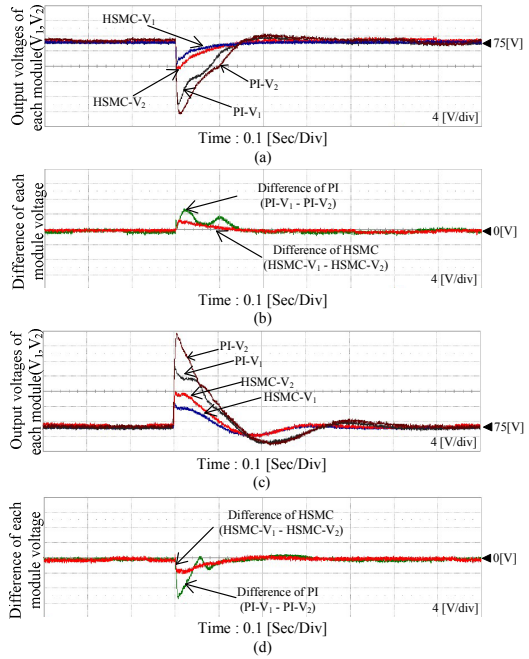

Fig. 8. Performance of module voltages for HSMC and PI contorl under difference inductance (L_2>L_1)., (a) Module voltages under load increase. (b) Difference for two contorllers under load decrease. (c) Module voltages under load increase. (d) Difference of two contorllers under load decrease.

two DAB modules. It is seen that d_1 and d_2 are different for the balancing control of output voltages of two DAB modules since the leakage inductances are set differently in this case.

Fig. 8 shows the performance comparison of the HSMC and PI control in transient state, where the load is changed from 380 W to 600 W and from 600 W to 380 W under different inductance condition of the individual modules (L_2 > L_1). Fig. 8(a) and (c) show the transient responses of individual module voltages for module #1 and #2. Fig. 8(b) and (d) show the voltage mismatches between module #1 and #2. In the PI control, the maximum voltage mismatches are about 5 V and 10 V when the load is increased and decreased, respectively. However, those of in the HSMC are just about 2 V and 4 V, respectively, under the same condition. As can be seen, the

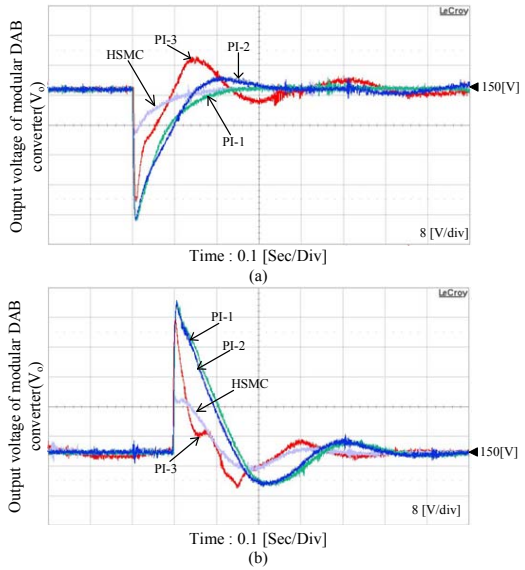

Fig. 9. Performance comparison of HSMC and PI control. (a) Load increase from 380 W to 600 W. (b) Load decrease from 600 W to 380 W.

HSMC shows less sensitivity to parameter mismatch than PI control.

Fig. 9 shows the performance comparison of the DC bus voltage responses of the HSMC and PI control in the cases of the load variations, which are changed from 380 W to 600 W and from 600 W to 380 W under unequal module inductance condition ($L_2 > L_1$). As can be seen, the HSMC gives a faster transient response without oscillations than the PI control.

V. CONCLUSIONS

In this paper a novel output voltage control and balancing scheme of the IPOS modular DAB DC/DC converter has been proposed without any additional controller for balancing . At first, a nonlinear modeling of the system has been derived and then the voltage controller has been designed based on the HSMC theory. The proposed HSM controller provides not only good balancing control performance but also the fast transient response even though the parameter mismatch between two converter modules exists. The validity of the proposed control scheme has been verified by experimental results for the reduced-scale converter system at laboratory.

ACKNOWLEDGMENT

This research was supported by Basic Science Research Program through the National Research Foundation of Korea (NRF) funded by the Ministry of Science, ICT and Future Planning (NRF-2014R1A2A1A11052748).

REFERENCES

[1] H. Fan, and H. Li, "High-Frequency Transformer isolated bidirectional DC–DC Converter modules with high efficiency over wide load range for 20 kVA Solid-State Transformer," IEEE Trans. on Power Electron., vol. 26, no. 12, pp. 3599-3608, Dec. 2011.

[2] FM. Bahmani, T. Thiringer, A. Rabiei, and T. Abdulahovic, "Comparative study of a multi-mw high power density dc transformer with an optimized high frequency magnetics in all-dc offshore wind farm," IEEE Trans. Power Del., vol. 31, no. 2, pp. 5738–5745, Apr. 2016.

[3] K. Sano and M. Takasaki, "A boost conversion system consisting of multiple DC-DC converter modules for interfacing wind farms and HVDC transmission," in Proc. of IEEE ECCE, 15-19 Sep. 2013, pp. 2613– 2618.

[4] F. Krismer, J. W. Kolar, "Efficiency-optimized high-current dual active bridge converter for automotive applications," IEEE Trans. Ind. Electron., vol. 59, no. 7, pp. 2745-2760, Jul. 2012.

[5] M. N. Kheraluwala, R. W. Gascoigne, D. M. Divan, and E. D. Baumann, "Performance characterization of a high-power dual active bridge," IEEE Trans. Ind. Appl., vol. 28, no. 6, pp. 1294-1301, 1992.

[6] Y. Tang and A. Khaligh, "Bidirectional hybrid battery/ultracapacitor energy storage systems for next generation MVDC Shipboard power systems," in Proc. of IEEE VPPC, 6-9 Sep. 2011, pp. 1–6.

[7] Y. C Jeung, and D. C. Lee, "Sliding mode control of bi-directional dual active bridge DC/DC converters for battery energy storage systems," in Proc. of APEC, 26-30 Mar. 2017. pp. 3385-3390.

[8] G. Xu, D. S. Shang, and X. Z. Liao, "Decentralized inverse-droop control for input-series-output-parallel DC–DC converters," IEEE Trans. Power Electron., vol. 30, no. 9, pp. 4621–4625, Sep. 2015.

[9] X. Yu, X. She, A. Huang and L. Liu, "Distributed power balance strategy for DC/DC converters in solid state transformer," in Proc. of IEEE APEC, 16-20 Mar. 2014, pp. 989-994.

[10] L. Qu, D. Zhang, and Z. Bao, "Active output-voltage-sharing control scheme for input series output series connected DC–DC converters based on a master slave structure," IEEE Trans. on Power Electron., vol. 32, no.8, pp. 6638-6651, Oct. 2016.

[11] Z. Guo, D. Sha, and X. Liao, "Input voltage sharing control for Input seriesoutput-parallel DC/DC converters without input voltage sensors," Journal of Power Electron., vol. 12, no. 1, pp. 83–87, Jan. 2012.

[12] D. Sha, Z. Guo, and X. Liao, "Cross-feedback output-current-sharing control for input-series-output-parallel modular DC-DC converters," IEEE Trans. on Power Electron., vol. 25, no. 11, pp. 2762–2771, Nov.2010.

[13] Q. Wei, B. Wu, D. Xu, and N. R. Zargari, " Model predictive control of capacitor voltage balancing for cascaded modular dc–dc converters," IEEE Trans. Power Electron., vol. 32, no. 1, pp. 752–761, Jan. 2017.

[14] R. W. A. A. D. Doncker, D. M. Divan, and M. H. Kheraluwala, "A three phase soft-switched high-power-density dc/dc converter for high-power applications," IEEE Trans. Ind. Appl., vol. 27, no. 1, pp. 63–73, Jan./Feb.1991.

[15] C. Mi, H. Bai, C.Wang, and S.Gargies, "Operation, design and control of dual H-bridge-based isolated bidirectional dc-dc converter," IET Power Electron., vol. 1, no. 4, pp. 507–517, Apr. 2008.

[16] D. Segaran, B. P. McGrath, and D. G. Holmes, "Adaptive dynamic control of a bi-directional dc-dc converter," in Proc. of IEEE ECCE, 12-16 Sep. 2010, pp. 1442–1449.

[17] J.-J. E. Slotine, W. Li, Applied Nonlinear Control. Prentice-Hall,1991.

[18] Y. Hao, J. Yi, D. Zhao, and D. Qian, "Robust control using incremental sliding mode for under actuated systems with mismatched uncertainties," in Proc. of American Control Conference, 11-13 Jun. 2008, pp. 532-537.

[19] S. C. Tan, Y. M. Lai, and C. K. Tse, Sliding Mode Control of Switching Power Converters - Techniques and Implementation. Boca Raton, FL,USA: CRC, 2012.

[20] W. Wang, J. Yi, D. Zhao, and D. Liu, "Design of a stable sliding-mode controller for a class of second-order under actuated systems," IET Control Theory Appl., vol. 151, no. 6, pp. 683–690, Nov. 2004.

[21] B. Liu, M. Yue, and R. Liu, "Motion control of an under actuated spherical robot: A hierarchical sliding-mode approach with disturbance estimation," in Proc. of ICMA, 2012 International Conference on, 5-8 Aug. 2012, pp. 1804-1809.